Polarimetric Atmospheric Imaging Radar (PAIR): Antenna Design, Testing, and Validation

José D. Díaz Díaz[†] ID
Advanced Radar Research Center
The University *of* Oklahoma
Norman Oklahoma, USA
jdiaz@ou.edu

David Schvartzman ID
Advanced Radar Research Center
The University *of* Oklahoma
Norman Oklahoma, USA
dschvart@ou.edu

Jorge L. Salazar-Cerreño ID
Advanced Radar Research Center
The University *of* Oklahoma
Norman Oklahoma, USA
salazar@ou.edu

Tian-You Yu ID
Advanced Radar Research Center
The University *of* Oklahoma
Norman Oklahoma, USA
tyu@ou.edu

Robert D. Palmer ID
Advanced Radar Research Center
The University *of* Oklahoma
Norman Oklahoma, USA
rpalmer@ou.edu

Matthew S. McCord ID
Advanced Radar Research Center
The University *of* Oklahoma
Norman Oklahoma, USA
mmccord@ou.edu

Abstract—Polarimetric phased array radars for weather applications require antennas with high co-polar beam matching and low cross-polarization levels to successfully estimate polarimetric meteorological products. In this communication, the authors present the design and validation of a dual-polarized, balanced probe-fed, stacked microstrip patch antenna operating in C-band (5.3 - 5.6 GHz) for the mobile Polarimetric Atmospheric Imaging Radar (PAIR), developed at the Advanced Radar Research Center (ARRC), University of Oklahoma (OU). The design of the antenna exploits balanced probe-fed feeding technique with thin dielectric substrates and low dielectric permittivities to suppress cross-polarized radiation. Simulation and measured results show scanning capabilities for -45° $\leq \theta \leq$ 45° and 0° $\leq \phi \leq$ 180° for all designed frequencies. Within the 3-dB width of the imaging beam intended to scan with PAIR, the antenna exhibits co-polar beam mismatch lower than 0.1 dB and cross-polarization levels under -40 dB, based on simulations and measured results.

Index Terms—balanced probe-fed, dual-polarized, intrinsic cross-polarization (IXR), low cross-polarization, microstrip antenna, phased array, polarimetric radar.

I. INTRODUCTION

The Polarimetric Atmospheric Imaging Radar (PAIR) is a revolutionary imaging phased array radar developed at the Advanced Radar Research Center (ARRC). Sponsored by the National Science Foundation, PAIR will serve as a scientific platform for studying rapidly-evolving severe weather [1]. Traditionally, imaging radars operate by transmitting a linearly polarized wide fan-beam in elevation while simultaneously receiving a number of narrow beams within the transmitted pattern using digital beam forming (DBF) [2], [3]. The PAIR system is rotated in azimuth while transmitting a wide dual-polarized fan-beam in elevation. Simultaneously, dual-polarized pencil beams are digitally formed in elevation within the transmitted pattern. As a dual-polarized phased array,

[†]José D. Díaz Díaz is now with the Johns Hopkins Applied Physics Laboratory (APL). Email: Jose.Diaz@jhuapl.edu

PAIR must comply with the polarimetric antenna requirements for weather measurements including: cross-polarization levels under -40 dB [4] and co-polarized beam mismatch under 0.1 dB [5] for all scanning angles and frequencies of the imaging beam (i.e., ± 20° in elevation).

In this paper, we present the design, testing, and validation of the PAIR phased array antenna which complies with the polarimetric antenna requirements for weather measurements. The performance of the antenna element is predicted by infinite array simulations of a unit-cell ran in Ansys HFSS. To test the antenna, mutual coupling measurements were obtained for a center element in an 8 x 8 antenna panel. The couplings are then used to estimate the active reflection coefficient across all frequencies and all pointing beam directions of interest. Furthermore, radiation pattern measurements were acquired in a far-field chamber for all elements in the antenna panel. These radiation patterns are then averaged to calculate an embedded element pattern. Finally, the simulated unit-cell and measured results are compared to validate the performance of the antenna.

II. ANTENNA DESIGN

The radiating element designed for the PAIR system is a balanced probe-fed microstrip patch antenna [6]. This antenna architecture requires two probes (or vias) connected to the microstrip patch for each polarization (i.e., horizontal or H, and vertical or V), needing only two metallic layers for integration. However, following this design approach alone will yield a limited operational bandwidth. To increase the bandwidth, the PAIR antenna must includes an extra metallic layer for a parasitic microstrip patch [7]. To balance and excite the H- and V-polarization signals, two extra metallic layers are needed: one for differential feeding each pair of probes [8] and another for a backing ground plane to allow planar integration [9].

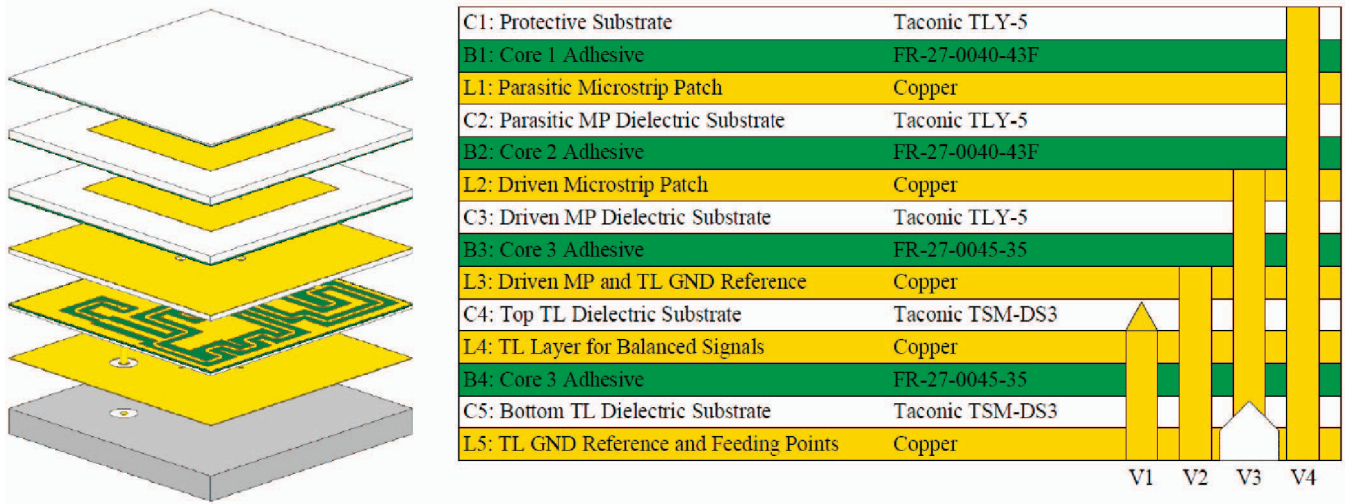| C1: Protective Substrate	Taconic TLY-5
B1: Core 1 Adhesive	FR-27-0040-43F
L1: Parasitic Microstrip Patch	Copper
C2: Parasitic MP Dielectric Substrate	Taconic TLY-5
B2: Core 2 Adhesive	FR-27-0040-43F
L2: Driven Microstrip Patch	Copper
C3: Driven MP Dielectric Substrate	Taconic TLY-5
B3: Core 3 Adhesive	FR-27-0045-35
L3: Driven MP and TL GND Reference	Copper
C4: Top TL Dielectric Substrate	Taconic TSM-DS3
L4: TL Layer for Balanced Signals	Copper
B4: Core 3 Adhesive	FR-27-0045-35
C5: Bottom TL Dielectric Substrate	Taconic TSM-DS3
L5: TL GND Reference and Feeding Points	Copper

Fig. 1. PAIR antenna unit-cell and stack-up with via configuration including all metallic layers for manufacturing and mounting plate. The manufacturing process requires sequential lamination. The probe locations are symmetric, with a distance from the center of the antenna of f_p = 4mm. The driven and parasitic microstrip patches are square with lengths L_p = 17.225 mm and L_{pp} = 16.575 mm. All stack-up thicknesses are given in mil: C1 - 5, B1 - 3.5, L1 - 1.4, C2 - 30, B2 - 3.5, L2 - 2, C3 - 30, B3 - 5.6, L3 - 2, C4 - 20, L4 - 1.4, B4 - 5.6, C5 = 10, L5 - 3.1. Note: C = Substrate, B = Prepreg, and L = Copper Layer. Note: V1 - controlled depth via, V2 - normal GND via, V3 - back-drilled via for signals, V4 - non-plated via for antenna mounting. Note 3: Electrical information about the dielectrics can be found in www.agc-multimaterial.com.

Fig. 1 shows the PAIR antenna unit-cell with the all metallic layers for manufacturing and its stack-up. The stack-up is made from low loss dielectric substrates and adhesives to maximize antenna efficiency, minimize surface waves, and reduce cross-polarization levels [10]. The radiating elements are excited with pogo pins (i.e., one for each polarization) that form a bridge between the RF electronics and the antenna Layer 5. The signals flow from these 50 Ω pins into the antenna feeding network present on Layer 4 through via #1. The feeding network is made from two reactive power dividers, highly isolated by grounding vias #2, each with an input and output impedance of 50 Ω. At the end of the reactive power dividers, the balanced signals leave through the back-drilled via #3, connecting to the driven patch on Layer 2 and bypassing the top antenna ground on Layer 3. To form the array panel, the unit-cell gets mirrored in both axes (i.e., x and y), forming a minimum replicable 2x2 subarray. This subarray then gets duplicated in both axes to form an 8 x 8 array antenna panel. Vias #4 are used in the corners of each unit-cell to mechanically attach the antenna to the electronics, forming a flushed connection with the system.

III. ANTENNA SIMULATIONS

An infinite array simulation for the PAIR antenna unit-cell was prepared in Ansys HFSS using periodic boundary conditions and Floquet-port analysis. Feedback from PCB and substrate manufacturers was obtained to depict with a high degree of confidence substrate thicknesses, plating tolerances, back-drilled via stubs, and other PCB inaccuracies that could be present in the final manufactured antenna panels. This feedback was then applied to the simulated PAIR antenna unit-cell. The simulation allowed for the calculation of the active
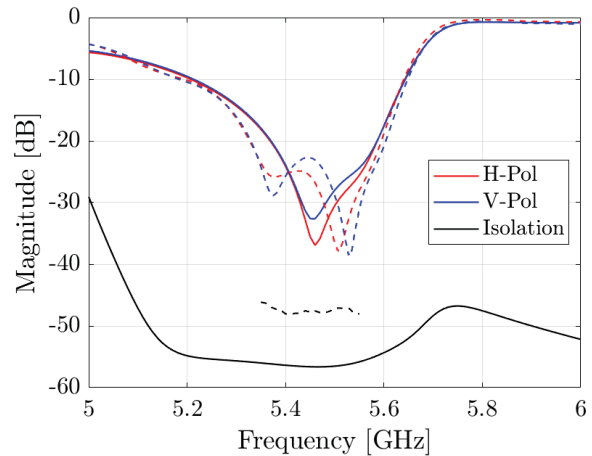

Fig. 2. Simulated (—) and measured (- -) active S-parameters of the PAIR antenna.

S-Parameters and its radiation patterns. More information regarding the antenna design can be found in [10].

A. Active S-Parameters

Fig. 2 show the expected active reflection coefficients of the antenna and its isolation at boresight. The overlap between the H- and V-curves show an exceptionally controlled impedance response, allowing operation from 5.3 to 5.6 GHz; within this frequency range, the isolation exceeds -50 dB. The scanned active reflection coefficients at 5.45 GHz (i.e., the designated center operating frequency) are shown in Fig. 3 and 4. It can
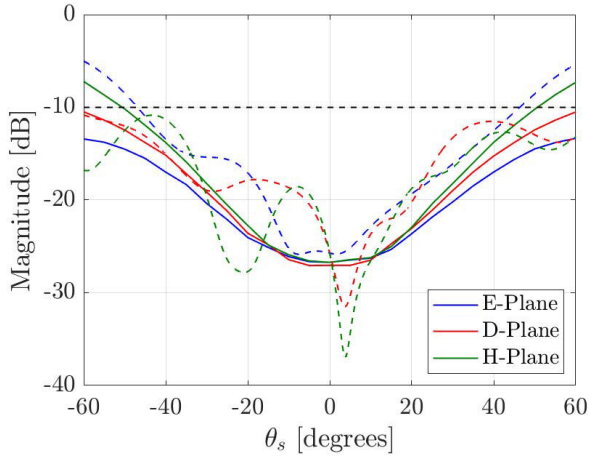
Fig. 3. Simulated (—) and measured (- -) scanned H-polarized active reflection coefficient of the PAIR antenna at 5.45 GHz.
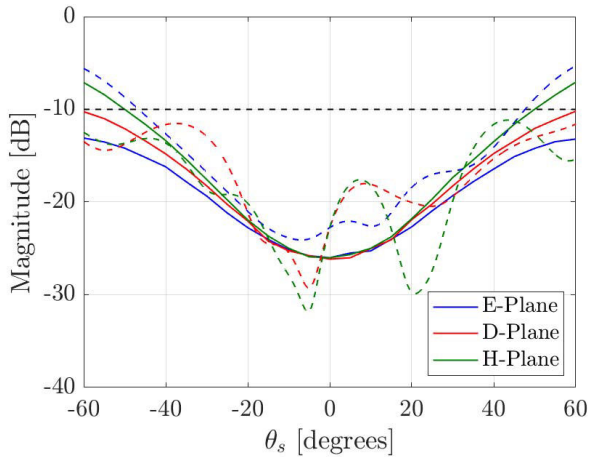

Fig. 5. Simulated (—) and measured (∘ ∘) H-polarized radiation patterns of the PAIR antenna at 5.45 GHz.

Fig. 4. Simulated (—) and measured (- -) scanned V-polarized active reflection coefficient of the PAIR antenna at 5.45 GHz.

Fig. 6. Simulated (—) and measured (∘ ∘) V-polarized radiation patterns of the PAIR antenna at 5.45 GHz.

be seen that the antenna maintains reflections for E-, D- and H-planes under -10 dB in $-45° \leq \theta \leq 45°$. These results show that the PAIR antenna is capable of scanning beyond the limits of the imaging beam, allowing it to be used in applications requiring a wide scanning range.

B. Radiation Patterns

Figs. 5 and 6 show the PAIR antenna radiation patterns in Ludwig's 3rd definition of polarization [11] at a frequency of 5.45 GHz for the H- and V-polarizations, respectively. According to the infinite array simulation results, the expected co-polarized beam mismatch between E- and H-planes of different polarizations is lower than 0.1 dB within the beamwidth of the imaging beams. This mismatch increases as a function of scanning direction, reaching a maximum of 0.21 dB at $\theta = \pm 45°$. The cross-polarization within the imaging beam is expected to be lower than -40 dB, reaching a maximum of -30 dB at $\theta = \phi = \pm 45°$. These simulation results show that the PAIR antenna should have the ability to estimate sufficiently accurate polarimetric weather
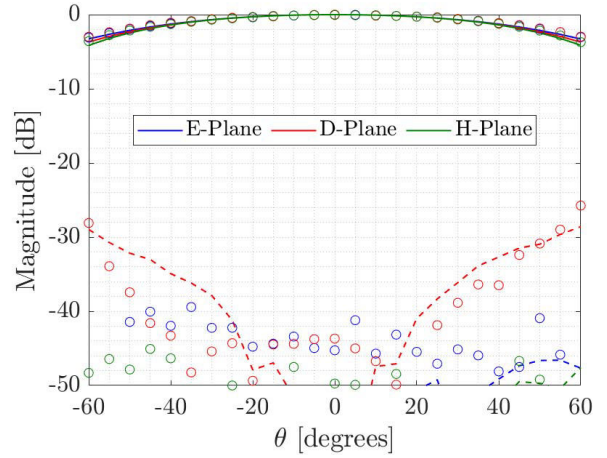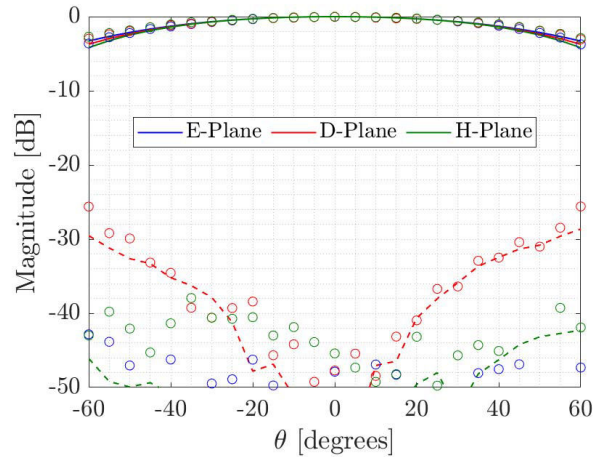
measurements without significant biases within the imaging beam.

Fig. 7 shows the intrinsic cross-polarization (IXR) for the antenna as defined in [12]. The IXR combines the co- and cross-polarization patterns of each polarization to estimate the worst-case, cross-polarization ratio before calibration. The IXR for the PAIR antenna is expected to be higher than 60 dB within the imaging beam, reaching a minimum of 38 dB at $\theta = \pm 45°$. These results are further evidence to support the polarization control that the PAIR antenna offers, even at wide scanning angles.

IV. ANTENNA MEASUREMENTS

The PAIR antenna was validated using two methods: first by S-parameter measurements with a network analyzer to examine the active reflection coefficient, and second, by measuring the radiation patterns of every element on the 8×8 panel in a far-field chamber (i.e., 128 measurements). In the first method, the couplings from one of the elements in the center of the antenna panel were acquired for both
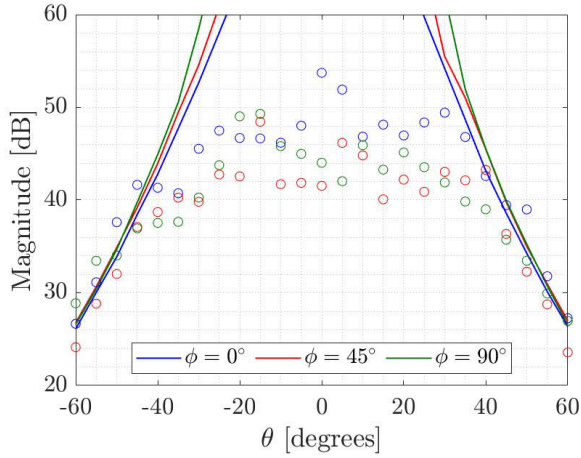
Fig. 7. Simulated (—) and measured (∘ ∘) intrinsic cross-polarization (IXR) of the PAIR antenna at 5.45 GHz for $\phi = 0°$, $45°$, $90°$.

polarizations. These couplings were measured from the H-port to all other H-polarization ports, and from the V-port to all other V-polarizations. In the second method, the co- and cross-polarized radiation patterns were measured in a far-field chamber in the ARRC, with a resolution of 5° in both θ and ϕ. The chamber operates between 2 and 26 GHz with a cross-polarization measurement capability of -35 dB. This is particularly important when analyzing the cross-polarization data acquired with the system.

A. Active S-Parameters

With the acquired S-parameter couplings, the active reflection coefficients for the H- and V-polarizations were calculated according to [13]. Fig. 2 shows the results at boresight across frequencies (dashed lines). The measured responses appear to be almost identical, agreeing also with simulation results in most of the bandwidth. It was not possible to derive an active S-parameter for the isolation. The reason for this lies on the H-V coupling levels (i.e., under -60 dB), making difficult to maintain the calibration of the network analyzer through the course of the measurements. Instead, isolation levels were estimated by averaging cross-polarization levels (between H and V) at boresight. These results show an averaged isolation of -47 dB within the operational bandwidth of the antenna.

Fig. 3 and 4 show the measured active reflection coefficient at 5.45 GHz for H- and V-polarization (dashed lines). It is seen that the antenna maintains scanned active reflections under -10 dB for E-, D-, and H-planes in $-45° \leq \theta \leq 45°$. Although not presented here, the scanned active reflections are maintained within the operational bandwidth of the antenna. The discrepancy between simulated and measured results is likely given by the size of the array (i.e., one 8×8 panel). To obtain more accurate results and better agreement with simulations, the size of the array has to be increased and more couplings must be measured. Nevertheless, in this work, the current results with the 8 × 8 panel are sufficient to validate the performance of the antenna.

B. Radiation Patterns

Fig. 5 and 6 show the normalized, averaged radiation patterns for H- and V-polarizations at 5.45 GHz (∘ ∘ markers), using 64 elements per polarization. The averaged patterns were calculated by spatially shifting all H- and V-pol measurements into the geometrical center of the 8 x 8 antenna panel. The observed co-polarized beam mismatch between polarizations is lower than 0.1 dB within the imaging beam. The mismatch increases to 0.23 dB at $\theta = \pm 45°$. In terms of cross-polarization, the averaged patterns show values under -40 dB within the imaging beam. The highest cross-polarization of the antenna occurs in the D-plane at $\theta = \pm 45°$, where simulation and measured results predict -30 dB. The noise in the averaged cross-polarization pattern can be explained by the averaging of low-level cross-pol magnitudes with highly dependent phase components. Fig. 7 show the IXR for the averaged radiation patterns calculated for H- and V-polarization (∘ ∘ markers). Within the imaging beam, the IXR rises above 40 dB, receding with scan angle to 35 dB at $\theta = \pm 45°$. When compared to simulations, the worst expected IXR is only 3 dB lower than simulations at $\theta = \pm 45°$. These results prove the ability of the PAIR antenna to maintain polarization control in and beyond its imaging beam.

V. CONCLUSIONS

This paper presents the design, testing, and validation of the PAIR antenna. The design exploits the balanced probe-fed feeding technique with thin dielectric substrates and low dielectric permittivities. The balanced probe-fed feeding technique allows for symmetrical performance between H- and V-polarizations. The thin dielectric substrates with low dielectric constants suppress scanned cross-polarized radiation and improves co-polarized beam matching. Simulated and measured results for the antenna show an operational bandwidth between 5.3 to 5.6 GHz; scanned active reflection coefficients under -10 dB for $-45° \leq \theta \leq 45°$ and $0° \leq \phi \leq 180°$; co-polarized beam mismatch under 0.1 dB within the imaging beam and 0.23 dB at $\theta = \phi = \pm 45°$. Cross-polarized radiation is under -40 dB within the imaging beam and -30 dB at $\theta = \phi = \pm 45°$. Further, the analysis using the averaged radiation patterns from the aperture yielded an IXR above 40 dB within the imaging beam and 35 dB at $\theta = \phi = \pm 45°$. It is reminded here that the anechoic chamber used in these measurements is rated for cross-polarization levels of -35 dB. This value is higher than the expected cross-polarization levels of the PAIR antenna. Thus, for more accurate measurements, the PAIR antenna requires a far-field system with better cross-polarization measurement capabilities. Nevertheless, the results shown here states that the PAIR antenna has the ability to retrieve polarimetric weather measurements with sufficient accuracy, mitigating polarimetric biases with its imaging beam.

ACKNOWLEDGMENT

REFERENCES

[1] J. L. Salazar et al., "An Ultra-Fast Scan C-band Polarimetric Atmospheric Imaging Radar (PAIR)," 2019 IEEE International Symposium on Phased Array System & Technology (PAST), 2019, pp. 1-5, doi: 10.1109/PAST43306.2019.9021042.

[2] B. Isom et al., "The Atmospheric Imaging Radar (AIR) for high-resolution observations of severe weather," 2011 IEEE RadarCon (RADAR), 2011, pp. 627-632, doi: 10.1109/RADAR.2011.5960613.

[3] D. Schvartzman & Others Distributed Beams: Concept of Operations for Polarimetric Rotating Phased Array Radar. *IEEE Trans. On Geoscience And Remote Sensing*. pp. 1-19 (2021)

[4] Y. Wang and V. Chandrasekar, "Polarization isolation requirements for linear dual-polarization weather Radar in simultaneous transmission mode of operation," in IEEE Transactions on Geoscience and Remote Sensing, vol. 44, no. 8, pp. 2019-2028, Aug. 2006, doi: 10.1109/TGRS.2006.872138.

[5] G. Zhang, "Weather Radar Polarimetry", 1st ed. Boca Raton, FL, USA: CRC Press, 2016, ch. 8, p. 258.

[6] J. Schuss and J. Hanfling, "Nonreciprocity and scan blindness in phased arrays using balanced-fed radiators," in IEEE Transactions on Antennas and Propagation, vol. 35, no. 2, pp. 134-138, February 1987, doi: 10.1109/TAP.1987.1144064.

[7] R. B. Waterhouse, "Design of probe-fed stacked patches," in IEEE Transactions on Antennas and Propagation, vol. 47, no. 12, pp. 1780-1784, Dec. 1999, doi: 10.1109/8.817653.

[8] C. Fulton and W. Chappell, "A dual-polarized patch antenna for weather radar applications," 2011 IEEE International Conference on Microwaves, Communications, Antennas and Electronic Systems (COMCAS 2011), 2011, pp. 1-5, doi: 10.1109/COMCAS.2011.6105940.

[9] J. A. Ortiz et al., "Ultra-compact universal polarization X-band unit cell for high-performance active phased array radar," 2016 IEEE International Symposium on Phased Array Systems and Technology (PAST), 2016, pp. 1-5, doi: 10.1109/ARRAY.2016.7832592.

[10] J. D. Diaz, "Ultra-low Cross Polarization Antenna Architectures for Multi-function Planar Phased Arrays", PhD dissertation, University of Oklahoma, Norman, OK, USA, 2021.

[11] A. Ludwig, "The definition of cross polarization," in IEEE Transactions on Antennas and Propagation, vol. 21, no. 1, pp. 116-119, January 1973, doi: 10.1109/TAP.1973.1140406.

[12] T. D. Carozzi and G. Woan, "A Fundamental Figure of Merit for Radio Polarimeters," in IEEE Transactions on Antennas and Propagation, vol. 59, no. 6, pp. 2058-2065, June 2011, doi: 10.1109/TAP.2011.2123862.

[13] D. M. Pozar, "A relation between the active input impedance and the active element pattern of a phased array," in IEEE Transactions on Antennas and Propagation, vol. 51, no. 9, pp. 2486-2489, Sept. 2003, doi: 10.1109/TAP.2003.816302.